J. Nanostruct Chem. 2026; 16(3): 304-318

Journal of Nanostructure in Chemistry (JNSC)

https://doi.org/10.57647/jnsc.2026.1603.15

Research Article

Zein–Lecithin Nanoparticle Encapsulation of *Eucommia ulmoides* Leaf Total Flavonoids: Controlled-Release Kinetics and Physicochemical Stability

Xin-yu Wang[1,*,#], Jian-wei Jiang[2,3,4#], Wen Wen[1#], Yong-li Ma[1], Min Wu[1]

[1]*Department of Pharmacy, Hangzhou TCM Hospital Affiliated to Zhejiang Chinese Medical University, Hangzhou, Zhejiang, 310007, China*
[2]*Department of Pharmacy, Zhejiang Cancer Hospital, Hangzhou, Zhejiang, 310022, China*
[3]*Hangzhou Institute of Medicine (HIM), Chinese Academy of Sciences, Zhejiang, 310018, China*
[4]*Integrated Traditional Chinese and Western Medicine Oncology Laboratory, Key Laboratory of Traditional Chinese Medicine of Zhejiang Province, Hangzhou, Zhejiang, 310022, China*
 # Xin-yu Wang, Jian-wei Jiang, and Wen Wen contributed equally to this work as co-first authors.

*** Corresponding authors:** wangxinyu0320@163.com; 2021b452@zcmu.edu.cn

Article History:

Received:
03 January 2025

Revised:
27 January 2026

Accepted:
04 February 2026

Published in Issue:
30 June 2026

Abstract

Total flavonoids from *Eucommia ulmoides* leaves (EUTF) show poor aqueous solubility and limited oral bioavailability, restricting their use in functional foods and pharmaceutical formulations. This work developed an oral nano-delivery system by encapsulating EUTF into zein–lecithin hybrid nanoparticles (ZL-EUTF-NPs) fabricated via anti-solvent co-precipitation and optimized by the zein:lecithin mass ratio. The optimized formulation (Z:L = 1:1) produced spherical nanoparticles with a mean hydrodynamic diameter of 155.2 ± 5.2 nm, PDI 0.18 ± 0.02, and zeta potential −35.6 ± 1.5 mV, consistent with a stable colloidal dispersion. Encapsulation efficiency and loading capacity reached 85.3 ± 2.1% and 8.5 ± 0.2%, respectively. FTIR, XRD, and DSC indicated that EUTF was molecularly dispersed in an amorphous state within the protein–lipid matrix through non-covalent interactions. In simulated gastrointestinal conditions, ZL-EUTF-NPs limited EUTF release to 14.2 ± 1.8% during 2 h in simulated gastric fluid (pH 1.2) and enabled sustained intestinal release, reaching 72.8 ± 3.1% after 10 h total incubation. Release in simulated intestinal fluid was best fitted by the Korsmeyer–Peppas model (R^2 = 0.995; n = 0.67), indicating anomalous (non-Fickian) transport governed by coupled diffusion and matrix erosion. The encapsulated EUTF retained high antioxidant activity (DPPH 82.1 ± 2.8%; ABTS 89.5 ± 3.0% at 50 μg/mL equivalent), while the nanocarrier showed low cytotoxicity (cell viability ≥85% across 10–200 μg/mL equivalent EUTF) and efficient time-dependent uptake in Caco-2 cells. Physicochemical stability testing showed minimal changes under refrigerated storage with 94.5 ± 2.6% flavonoid retention after 90 days at 4°C. Overall, zein–lecithin hybrid nanoparticles provide a practical strategy to enhance EUTF stability and modulate intestinal release for oral applications.

Keywords: Eucommia ulmoides leaf flavonoids; Nanoencapsulation; Controlled release; Physicochemical stability; Zein-lecithin nanoparticles

Cite this article: Xin-yu W., Jian-wei J., Wen W., Yong-li M., Min W. Zein–Lecithin Nanoparticle Encapsulation of *Eucommia ulmoides* Leaf Total Flavonoids: Controlled-Release Kinetics and Physicochemical Stability. *J Nanostruct Chem* **16**, 304-318 (2026). https://doi.org/10.57647/jnsc.2026.1603.15

1. Introduction

Eucommia ulmoides Oliv. is a deciduous tree native to China. Due to its extensive therapeutic properties, it has been used in traditional medicine for centuries [1]. Its leaves are a particularly rich source of bioactive compounds, including iridoids, lignans and polysaccharides, with total flavonoids (EUTF) being one

of the most important functional components [2]. These flavonoids mainly include compounds such as rutin, kaunferol and quercetin, which have been proven to have powerful biological activities, including strong antioxidant, anti-inflammatory, liver-protective and neuroprotective effects [3].The antioxidant properties of EUTF, often found to be superior to those of synthetic antioxidants like vitamin C in various assays, are attributed to their ability to effectively scavenge free radicals such as DPPH, ABTS, and hydroxyl radicals [4]. These properties make EUTF highly valuable for the prevention and management of oxidative stress-related chronic diseases [5].Despite their promising therapeutic potential, the practical application of EUTF in functional foods, nutraceuticals, and pharmaceuticals is severely hampered by several inherent physicochemical limitations [6]. The primary challenge is their extremely poor water solubility, which leads to low oral bioavailability and limits their systemic absorption after ingestion [7]. Furthermore, flavonoids are susceptible to degradation under the harsh conditions of the gastrointestinal (GI) tract, including extreme pH values and enzymatic activity, as well as during food processing and storage, which further diminishes their efficacy [8]. In order to overcome these obstacles, people have explored various strategies, among which nano-encapsulation has become a particularly effective method. Encapsulating bioactive compounds within nanocarriers can enhance their solubility and dispersibility in aqueous media, protect them from degradation, control their release at specific sites in the body, and improve their cellular uptake, thereby increasing overall bioavailability and therapeutic effectiveness. Zein, the primary storage protein extracted from corn, has received considerable interest among the biopolymers utilized for nanoencapsulation. [9]. Corn protein is listed as recognized as safe (GRAS) by the U.S. Food and Drug Administration, and is known for its biocompatibility, biodegradability and unique amphrinity[10]. High proportion of non-polar amino acids enables its solubility in aqueous ethanol while remaining insoluble in water [11]. a property that allows for the straightforward fabrication of nanoparticles via methods like anti-solvent precipitation [12]. This technique involves dissolving zein and a hydrophobic bioactive in an aqueous-organic solvent and then introducing this solution into an anti-solvent (typically water), causing the zein to self-assemble into nanoparticles and entrap the bioactive compound within its hydrophobic core [13].

Although zein–lecithin hybrid/composite nanoparticles have been explored for improving the dispersibility, stability, and gastrointestinal-stage delivery of selected polyphenols, the existing evidence base is still largely built on model single compounds rather than chemically complex botanical flavonoid mixtures [14]. For example, zein–lecithin composite nanoparticles prepared via antisolvent co-precipitation have been reported to stabilize hydrophobic polyphenols such as curcumin through protein–phospholipid assembly and to improve colloidal robustness relative to zein alone [15]. In addition, zein–lecithin nanocomplexes have shown distinct stage-dependent release behavior during simulated gastrointestinal digestion, with limited release in simulated gastric fluid but substantially higher cumulative release in simulated intestinal fluid for polyphenolic payloads (e.g., EGCG). However, *Eucommia ulmoides* leaf total flavonoids (EUTF) represent a multicomponent flavonoid system with broad polarity distribution and multiple interaction motifs, and their application is still limited by poor water solubility and associated bioavailability constraints [16]. Under this context, at least three research gaps remain insufficiently addressed: (i) systematic formulation optimization and structure–property mapping for zein–lecithin carriers loaded with *complex flavonoid mixtures* rather than single standards; (ii) mechanistic controlled-release kinetics analysis in simulated GI environments with appropriate model fitting to clarify transport behavior for multicomponent payloads; and (iii) longer-term physicochemical stability evaluation (beyond short-term dispersion checks) to support realistic storage and functional-food/pharmaceutical translation [17].

However, as far as we know, there is a lack of systematic research on the development of corn phospholipid hybrid nanoparticles of total flavonoids in Eucommia leaves. Comprehensive data on the formulation optimization, detailed physicochemical characterization, controlled-release kinetics in simulated GI conditions, and long-term stability of such a system have not yet been reported. This study aims to fill this knowledge gap. We hypothesize that encapsulating EUTF within an optimized zein-lecithin nanoparticle matrix will significantly improve its physicochemical stability and provide a sustained release profile suitable for oral delivery. The objectives of this research were to: (1) prepare and optimize EUTF-loaded zein-lecithin nanoparticles (ZL-EUTF-NPs) using an anti-solvent co-precipitation method; (2) conduct extensive material characterization using a range of microscopic and spectroscopic techniques; (3) investigate the in vitro release profile and kinetic mechanisms under simulated GI conditions; and (4) evaluate the antioxidant activity, cytotoxicity, cellular uptake, and long-term physicochemical stability of the developed nanocarriers.

2. Materials and Methods

2.1. Materials

Corn protein (from corn, >90% protein), soybean lecithin (>95% phosphatidylcholine), porcine gastric mucosal

10.57647/jnsc.2026.1603.15

pepsinase (≥250 units/mg), porcine pancreatic pancreatin (8 times USP specification) and bile salt purchased from Sigma-Aldrich (St. Louis, MO, USA).

Eucommia is harvested from an organic farm in Shaanxi Province, China, and has been certified by the pharmacy classroom of Beijing traditional Chinese medicine students.

Rutin standard products (purity ≥98%, HPLC grade), 2,2-diphenyl-1-pyridine (DPPH) and 2,2'-nitro-bis (3-ethylbenzothiazole-6-sulfonic acid) (ABTS) are provided by Shanghai Aladdin Biochemical Technology Co., Ltd. in China.

Acetonitrile and formic acid (HPLC grade) are purchased from Fisher Scientific (Waltham, MA, USA). Gibco (Grand Island, NY, USA) provides Dulbecco's Modified Eagle culture medium (DMEM), fetal bovine serum (FBS), penicillin-streptomycin and cell counting kit-8 (CCC-8 Caco-2 human colorectal cancer cell lineage comes from American type culture collection (ATCC, Manassas, VA, USA).

All other chemicals and reagents are analytical grade and can be used without further purification. Deionized water was used throughout the experiment.

2.2. Extraction and Quantification of *Eucommia ulmoides* Total Flavonoids (EUTF)

The dried euonymus leaves are ground into fine powder. The powder (100 g) is extracted in a 60°C ultrasonic bath for 60 minutes with a 70% (v/v/v) ethanol aqueous solution (1:20 w/v).

This process has been repeated three times. Combine, filter and concentrate the extracted liquid under reduced pressure. Then use the previously described polyamide column chromatography method to purify the crude extract and slightly modify it [18].

Collect the purified EUTF powder and store it at -20°C for subsequent use. Use an Agilent 1260 Infinity II HPLC system with a diode array detector (DAD) from Agilent Technologies in Santa Clara, CA, USA, to measure the total flavonoid content.

A Zorbax Eclipse Plus C18 chromatography column (4.6 × 250 mm, 5 μm) is employed, with the temperature set at 30°C. The mobile phase consists of 0.1% (v/v) formic acid in water (A) and acetonitrile (B). The gradient elution program is configured as follows: 15% B from 0-5 min, increased to 40% B over 5-25 min, reduced back to 15% B during 25-30 min, and maintained at 15% B from 30-35 min. The detection wavelength is set at 354nm, with a flow rate maintained at 1.0 mL/min [19].

Use rutin as the external standard for quantification. The calibration curve, expressed as $y = 25843x + 105.7$, shows a strong linear relationship within the 5-100 μg/mL range ($R^2 = 0.9996$), where y denotes the peak area and x indicates the concentration in μg/mL.

2.3. Preparation of Zein–Lecithin–EUTF Nanoparticles (ZL-EUTF-NPs)

ZL-EUTF-NPs were prepared by an improved anti-solvent co-precipitation method. In the standard process, 100 mg corn protein and 10 mg EUTF are mixed with 10 mL 70% (v/v) of ethanol aqueous solution to make the core solution. Dissolve lecithin in 10 mL of 70% ethanol in different amounts to prepare the shell solution. Corn protein and lecithin are combined with different mass ratios (1:0,4:1,2:1,1:1 and 1:2), while maintaining the same total polymer concentration to optimize the formula. After adding the lecithin solution, mix the corn protein-eutf solution well. At room temperature, stir at 800 rm/minute, and slowly add the final organic phase (20 mL) to 80 mL of DI water. The suspension is stirred under the ventilation cabinet for more than 4 hours, so that the ethanol is completely evaporated and the nanoparticles are self-assembled. Empty ZL-NPs are prepared by the same method, without EUTF. Preserve the nanoparticle suspension at 4°C for further analysis. Some of the optimized formulas are freeze-dried for solid-state characterization.

2.4. Characterization of Nanoparticles

2.4.1. *Particle Size, Polydispersity Index (PDI), and Zeta Potential*

At 25°C, the Zetasizer Nano ZS90 (Malvern Instruments, Malvern, UK) is employed to determine the average particle size, PDI, and zeta potential of nanoparticle suspensions using dynamic light scattering (DLS). To avoid multiple scattering effects, dilute the sample 100 times using deionized water before taking measurements.

2.4.2. *Encapsulation Efficiency (EE) and Loading Capacity (LC)*

The indirect method is used to determine both EE and LC. Centrifuge the freshly prepared ZL-EUTF-NP suspension (2 mL) at 15,000 × g for 30 minutes at 4°C. Gently gather the supernatant with free unsealed EUTF, and measure the flavonoid concentration using the high-performance liquid chromatography outlined in Section 2.2. The formulas for calculating EE and LC are presented as follows [20]:

EE (%) = [(Total amount of EUTF - Amount of free EUTF) / Total amount of EUTF] × 100

LC (%) = [(Total amount of EUTF - Amount of free EUTF) / Total weight of nanoparticles] × 100

2.4.3. *Morphological and Topographical Analysis*

Use transmission electron microscopy (TEM; JEEM-2100, JEOL, Tokyo, Japan) and scanning electron

10.57647/jnsc.2026.1603.15

microscopy (SEM; SU8010, Hitachi, Tokyo, Japan) to conduct detailed morphological analysis of the optimized ZL-EUTF-NPs. For TEM analysis, the nanoparticle suspension was diluted and placed on a carbon-coated copper grid, stained with 2% (w/v) phosphotungstic acid, and subsequently air-dried under an acceleration voltage of 200 kV[21]. For scanning electron microscopy analysis, the nanoparticles are first freeze-dried, and then placed on the aluminum root with double-sided tape. A thin layer of gold was splashed for 60 seconds before imaging at an accelerated voltage of 5 kV [22]. Surface geometry reveals the outward success of the assembly process. A Dimension Icon atomic force microscope scans surface shapes in tapping mode. Applying a diluted liquid to freshly split mica creates a clear observation field. Natural drying preserves the integrity of the layer. High-resolution imagery provides evidence of uniform particle size and distribution.

2.4.4. *Fourier Transform Infrared (FTIR) Spectroscopy*

Molecular fingerprints define the chemical environment of the carrier system. The Nicolet iS50 spectrometer scans frequencies from 4000 to 400 cm^{-1} with 4 cm^{-1} precision. Testing covers EUTF, corn protein, lecithin, and the physical blend alongside the freeze-dried nanoparticles. Fine powder combined with potassium bromide forms a solid disk under high pressure. Analyzing infrared patterns identifies potential bonding between components. Variations in peak positions signal the creation of new chemical bridges within the structure [23].

2.4.5. *X-ray Diffraction (XRD) and Differential Scanning Calorimetry (DSC)*

Crystalline arrangements and thermal transitions reveal the internal stability of the particles. A D8 Advance diffractometer generates X-rays at 40 kV and 40 mA via a copper source. Recording angles from 5°-60° at a pace of 2° per minute yields detailed diffraction maps. Diffraction patterns clarify the physical state of the encapsulated cargo [24]. A loss of sharp peaks suggests a shift from a crystalline to an amorphous form. Complementary thermal data comes from a Q2000 DSC unit. Small portions of material, roughly 3 to 5 mg, rest inside sealed aluminum pans. Heating from 25°C to 300°C at 10°C per minute reveals critical transition points. Continuous nitrogen flow prevents oxidation during the test. Monitoring energy changes confirms the successful integration of EUTF into the lipid-protein matrix [16].

2.5. In Vitro Release Study

Use dialysis bag method to evaluate the in vitro release of nanoparticle EUTF in simulated gastrointestinal condition [25]. Release study is performed in two parts: first in simulated gastric fluid (SGF, 0.1M HCl, pH 1.2, 0.32% w/v pepsin) and then in simulated intestinal fluid (SIF, 0.05M phosphate buffer, pH 6.8, 1% w/V pancreatic enzyme and 0.5% w/v bile salt). Put 5ml of ZL-EUTF-NP suspension (control is free EUTF solution)into dialysis bag(MWCO8-14kDa). Place in a 100mL of SGF. Incubate the bag with a shaker set to 37ºC (100 rpm) for 2 h. After 2 hrs, move bag to a 100-ml prewarmed SIF, and incubate for 8 hrs. At a certain time interval (0.5, 1, 1.5, 2 h in SGF; 2.5, 3, 4, 8, 10 h in SIF) take out 2ml of release medium, then add the same volume of fresh preheating medium to maintain precipitation condition. In the sample, the number of the EUTF was obtained by HPLC.

2.6. Release Kinetics Modeling

In order to clarify the release mechanism of EUTF in SIF, the cumulative release data is fit into 4 mathematical models [26]:

1.Zero-order model: $Q_t = k_0 t$

2.First-order model: $\ln(Q_\infty - Q_t) = \ln(Q_\infty) - k_1 t$

3.Higuchi model: $Q_t = k_n t^{1/2}$

4.Korsmeyer–Peppas model: $Q_t/Q_\infty = kt^n$

Among them, Q_t represents the cumulative drug release at t moments, Q_∞ represents the total release at infinite moments, and k_0, k_1, k_n and k represent the specific release rate constants of each model. In the Korsmeyer-Peppas model, the release index n reflects the release mechanism of the drug.

2.7. Antioxidant Activity Assays

The antioxidant activity of free EUTF and ZL-EUTF-NPs [27] was evaluated using the DPPH and ABTS radical scavenging assays, which are rapid and widely used methods to quantify electron- or hydrogen-donating capacity of antioxidants. In the DPPH assay, the reaction mixture was prepared by mixing an equal volume of sample solution (free EUTF solution or ZL-EUTF-NP dispersion, adjusted to an equivalent EUTF concentration of 50 μg/mL) with DPPH working solution prepared in ethanol. The blank control consisted of an equal volume of DPPH working solution mixed with ethanol (i.e., without sample), while the sample control consisted of an equal volume of sample solution mixed with ethanol without DPPH (i.e., to account for any intrinsic absorbance/scattering of the sample matrix). After incubation for 30 min in the dark at room temperature, absorbance was measured at 517 nm. In the ABTS assay, ABTS•+ was generated following a standard approach (oxidation of ABTS to form the radical cation), and the ABTS•+ working solution was then mixed with an equal volume of sample solution for analysis; the blank control consisted of ABTS•+ working solution mixed with the

10.57647/jnsc.2026.1603.15

corresponding solvent/buffer without sample, and the sample control consisted of sample solution mixed with the corresponding solvent/buffer without $ABTS^{\bullet+}$. After 6 min of reaction, absorbance was measured at 734 nm. Empty ZL-NPs were tested in parallel as a carrier control. Scavenging activity was calculated as Scavenging Activity (%) = $[(A_{blank} - A_{sample})/A_{blank}] \times 100$, where A_{blank} is the absorbance of the blank control (radical solution plus solvent), and A_{sample} is the absorbance of the radical solution mixed with sample; when sample background was non-negligible, the sample-control absorbance (sample without radical) was used to correct A_{sample} accordingly.

These two assays are complementary for encapsulation systems: DPPH uses a stable radical in an organic medium and is convenient for screening radical scavenging capacity, while $ABTS^{\bullet+}$ is applicable in both aqueous and organic environments and can be used to evaluate a broader range of antioxidant behaviors [28]. Together, they provide a practical assessment of whether encapsulation preserves antioxidant function and whether the antioxidant components remain accessible in the nanoparticle dispersion [29].

2.8. In Vitro Cytotoxicity and Cellular Uptake

CCK-8 method [30] detects the cytotoxicity of free EUTF, empty ZL-NPs and ZL-EUTF-NPs to Caco-2 cells. The cells are plated in a 96-hole plate with a density of 1×10^4 cells per hole and incubated for 24 hours. Then replace the culture medium with a fresh culture medium containing continuously diluted samples, with an equivalent EUTF concentration range of 10 to 200μg/mL. After 24 hours of incubation, CCK-8 reagents are added to each hole to measure the absorbance at 450nm wavelength. Compared with the untreated cells in the control group, cell vitality is expressed as a percentage.

In cell uptake research, coumarin-6 was used as a fluorescent probe to replace EUTF. Inoculate Caco-2 cells on the 6-hole plate on the glass cover. After reaching 80% fusion, the cells incubate with ZL-NPs (coumarin-6 concentration is 1μg/mL) loaded with coumarin-6 for 0.5, 2 and 4 hours. Then the cells are cleaned, fixed, and nuclear anti-stained with DAPI. Use a fluorescence microscope (Leica DMI8, Wetzlar, Germany) to observe cell uptake. After incubating cells at the same time as fluorescent nanoparticles, quantitative intake was evaluated by flow cytometer (BD FACSCanto II, BD Biosciences, San Jose, CA, USA).

2.9. Physicochemical Stability Study

The optimised ZL-EUTF-NPs evaluates their long-term stability by storing water dispersions and freeze-dried powders at different temperatures: samples are stored for 90 days at 4°C (refrigerated), 25°C (room temperature) and 40°C (acceleration conditions) respectively [31]. Check the physical appearance changes of the sample at the specified time points (0, 15, 30, 60 and 90 days), including aggregation and sedimentation, as well as particle size, PDI, zeta potential and flavonoid retention rate. The flavonoid retention rate is determined by calculating the percentage of EUTF that is still enclosed compared with the initial amount of day 0. Because this study aimed to isolate the effect of temperature, humidity and light exposure were not independently controlled or challenged; comprehensive stability profiling under ICH-style humidity and photostability conditions is therefore proposed as future work.

3. Results and Discussion

3.1. Optimization of ZL-EUTF-NP Formulation

The optimization of ZL-EUTF-NPs involved a systematic examination of the zein:lecithin (Z:L) mass ratio and the initial EUTF loading concentration. The anti-solvent precipitation method, based on the differential solubility of zein, was demonstrated to be a straightforward and efficient approach for nanoparticle fabrication [32]. The Z:L mass ratio plays a key role in controlling the self-assembly process and determining the final properties of the hybrid nanoparticles. We created five formulations, maintaining constant biopolymer and EUTF concentrations, with Z:L ratios set at 1:0 (pure zein), 4:1, 2:1, 1:1, and 1:2. Table 1 summarizes the results of particle size, PDI, zeta potential, EE, and LC, while Fig. 1 provides a visual representation of these findings.

The pure zein nanoparticles (Z:L ratio 1:0) exhibited a particle size of 248.6 ± 8.3 nm, which is relatively large, and a PDI of 0.31 ± 0.03, suggesting moderate polydispersity. Under pH ~6.0 conditions, the zeta potential was recorded at +12.4 ± 1.1 mV, slightly positive, which corresponds to the known isoelectric point (pI) of zein, generally around 6.2, indicating limited surface charge and implying weak colloidal stability that may lead to particle aggregation [33].

The addition of lecithin, an anionic phospholipid, significantly influenced all the parameters that were measured. With the increase in lecithin proportion, the particle size first dropped to a minimum of 155.2 ± 5.2 nm at a Z:L ratio of 1:1, then rose slightly to 168.9 ± 6.1 nm at a 1:2 ratio.

The initial reduction is likely due to lecithin's surfactant effect, which coats the surface of newly formed zein aggregates, thereby inhibiting their further growth and coalescence [34]. The slight rise at the maximum lecithin concentration might result from a thicker lecithin layer or increased incorporation of lecithin molecules into the particle structure [35].

10.57647/jnsc.2026.1603.15

The addition of lecithin caused a notable decrease in the PDI value, which measures size distribution homogeneity, reaching a minimum of 0.18 at the 1:1 ratio from an initial 0.31, suggesting the creation of a more consistent and monodisperse nanoparticle group [36]. The zeta potential shifted from positive to highly negative values, reaching -35.6 ± 1.5 mV at the 1:1 ratio. The reversal of charge verifies that lecithin molecules effectively adsorbed and formed a coating on the surface of the zein nanoparticles, introducing a significant negative charge that improves colloidal stability via electrostatic repulsion [37]. A zeta potential exceeding 30 mV in magnitude is typically regarded as a sign of exceptional long-term stability [38].

The addition of lecithin significantly enhanced both the encapsulation efficiency (EE) and loading capacity (LC). The encapsulation efficiency (EE) rose from 54.7 ± 3.5% for pure zein nanoparticles to a maximum of 85.3 ± 2.1% in the 1:1 formulation. Likewise, the LC increased from 5.5 ± 0.4% to 8.5 ± 0.2%. The enhancement results from the synergistic interaction among zein, lecithin, and the hydrophobic EUTF. The lecithin layer serves as a physical barrier to prevent drug leakage while also establishing a more lipophilic environment within the nanoparticle matrix, enhancing the entrapment of hydrophobic flavonoids via stronger hydrophobic interactions [8]. A Z:L mass ratio of 1:1 was selected as the optimal formulation for subsequent experiments because it resulted in the smallest particle size, lowest PDI, highest zeta potential magnitude, and greatest encapsulation efficiency. To determine the maximum drug loading capacity, different initial amounts of EUTF (5, 10, 15, and 20 mg, corresponding to EUTF:biopolymer mass ratios of 1:40, 1:20, 1:13.3, and 1:10) were used while keeping the optimal Z:L ratio of 1:1. The results are shown in Table 2 and Fig. 2. As the initial EUTF concentration increased, the particle size grew progressively from 145.1 nm to 180.5 nm. This is an expected phenomenon, as a higher amount of encapsulated material leads to a more compact and larger nanoparticle core [39]. The EE showed an interesting trend: it increased initially from 81.2% to 85.3% when the EUTF amount was raised from 5 to 10 mg but then slightly decreased to 82.5% and 78.4% at higher loadings. This suggests that the nanoparticle system has a saturation capacity; beyond a certain point (10 mg EUTF), the biopolymer matrix cannot efficiently entrap the excess drug, leading to a lower encapsulation efficiency [40]. In contrast, the loading capacity (LC) consistently increased with the initial EUTF amount, reaching a maximum of 11.8 ± 0.5% at the highest concentration. For subsequent studies, the formulation with 10 mg of EUTF was chosen, as it provided the best balance of high EE and a reasonably high LC without a significant increase in particle size.

Table 1. Effect of zein:lecithin (Z:L) mass ratio on the physicochemical properties of ZL-EUTF-NPs (mean ± SD, n=3)

Z:L Ratio	Particle Size (nm)	PDI	Zeta Potential (mV)	EE (%)	LC (%)
1:0	248.6 ± 8.3	0.31 ± 0.03	+12.4 ± 1.1	54.7 ± 3.5	5.5 ± 0.4
4:1	189.4 ± 7.2	0.25 ± 0.02	-18.9 ± 1.8	72.1 ± 2.8	7.2 ± 0.3
2:1	165.7 ± 5.9	0.20 ± 0.02	-29.5 ± 2.0	81.5 ± 1.9	8.2 ± 0.2
1:1	155.2 ± 5.2	0.18 ± 0.02	-35.6 ± 1.5	85.3 ± 2.1	8.5 ± 0.2
1:2	168.9 ± 6.1	0.21 ± 0.03	-38.2 ± 1.7	86.1 ± 2.5	8.6 ± 0.3

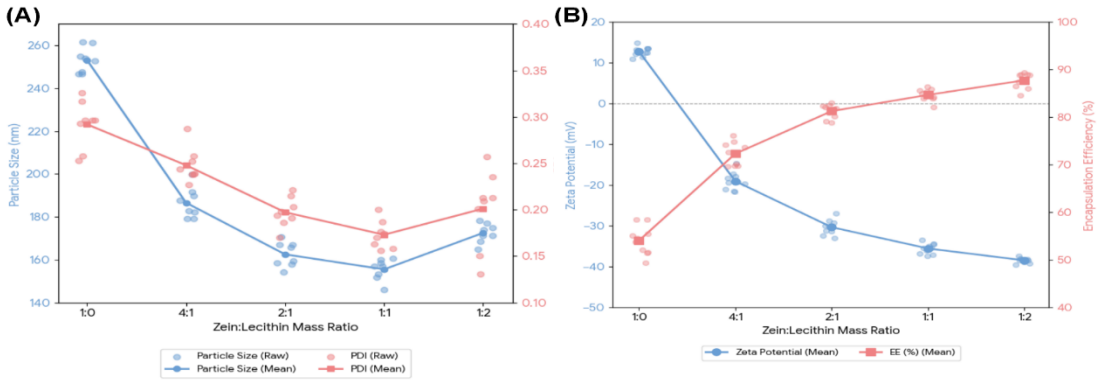

Figure 1. Impact of the zein:lecithin (Z:L) mass ratio on (A) Particle size and PDI, and (B) Zeta potential and Encapsulation Efficiency (EE) of ZL-EUTF-NPs. Results are shown as mean ± SD (n=3)

Table 2. Effect of initial EUTF loading on the properties of ZL-EUTF-NPs with a Z:L ratio of 1:1 (mean ± SD, n=3)

Initial EUTF (mg)	Particle Size (nm)	PDI	EE (%)	LC (%)
5	145.1 ± 4.8	0.17 ± 0.01	81.2 ± 2.5	4.1 ± 0.1
10	155.2 ± 5.2	0.18 ± 0.02	85.3 ± 2.1	8.5 ± 0.2
15	169.8 ± 6.5	0.22 ± 0.02	82.5 ± 2.9	10.3 ± 0.4
20	180.5 ± 7.1	0.26 ± 0.03	78.4 ± 3.3	11.8 ± 0.5

10.57647/jnsc.2026.1603.15

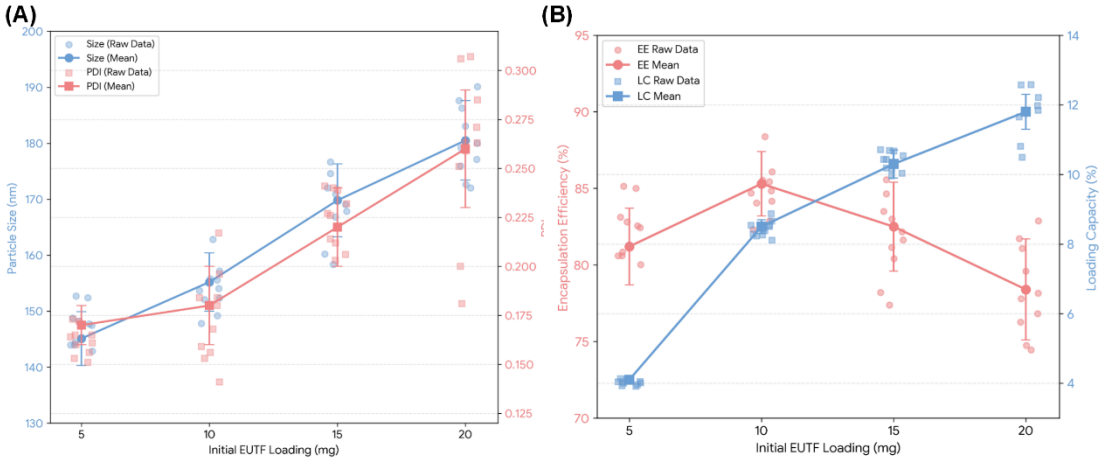

Figure 2. Impact of initial EUTF loading on (A) Particle size and PDI, and (B) EE and Loading Capacity (LC) of ZL-EUTF-NPs (Z:L ratio = 1:1). The data are shown as mean ± SD (n=3)

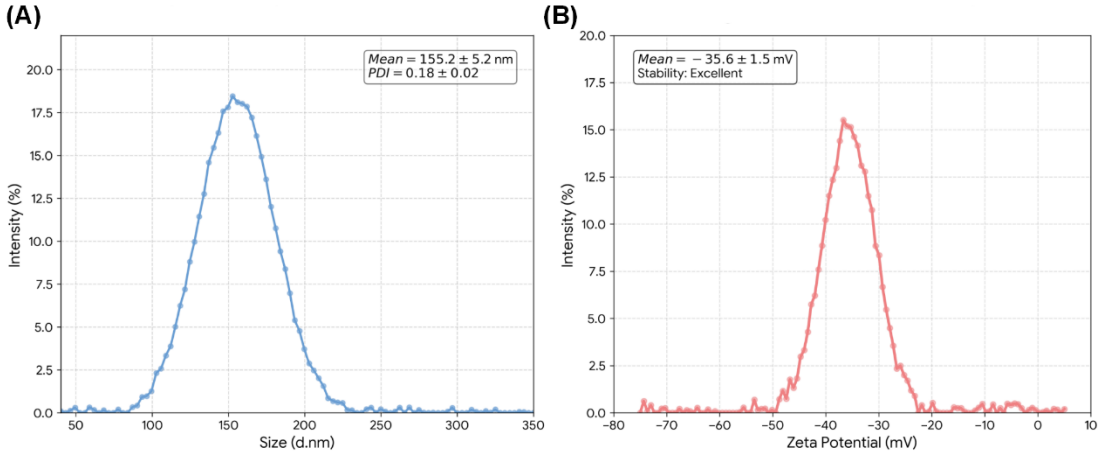

Figure 3. (A) Particle size distribution and (B) Zeta potential distribution of the optimized ZL-EUTF-NPs as measured by DLS

3.2. Physicochemical Characterization of Optimized ZL-EUTF-NPs

The optimized ZL-EUTF-NPs (Z:L ratio 1:1, 10 mg EUTF) were subjected to extensive characterization.

DLS analysis of the optimized formulation revealed a unimodal size distribution with a mean hydrodynamic diameter of 155.2 ± 5.2 nm and a low PDI of 0.18 ± 0.02 (Fig. 3A). The small size is advantageous for oral delivery as it can increase the surface area for dissolution and potentially enhance absorption across the intestinal epithelium. The low PDI value confirms the homogeneity of the nanoparticle suspension. The zeta potential was measured to be -35.6 ± 1.5 mV (Fig. 3B), indicating a highly stable colloidal dispersion resistant to aggregation due to strong inter-particle electrostatic repulsion. This negative charge is attributed to the orientation of the anionic phosphate groups of lecithin towards the outer aqueous phase [41].

The optimized ZL-EUTF-NPs were imaged using various techniques to observe their morphology. The TEM images in Fig. 4A showed spherical nanoparticles that were evenly dispersed, exhibiting no evidence of aggregation. The measured size matched the DLS results. At higher magnification (Fig. 4B), a distinct core-shell structure could be discerned, characterized by a darker core (zein and EUTF) and a lighter, less electron-dense surrounding layer (lecithin), which is in agreement with the proposed formation mechanism [42]. SEM analysis (Fig. 4C) of the lyophilized powder further confirmed the uniform, spherical morphology of the particles with smooth surfaces.

Fig. 5 illustrates the application of FTIR to observe the interactions between components within the nanoparticle matrix. The pure zein spectrum showed distinct peaks for amide I (C=O stretching) and amide II (N-H bending) at 1651 cm-1 and 1539 cm-1, respectively.

Lecithin exhibited peaks at 2924 cm-1 and 2854 cm-1 (C-H stretching of acyl chain), 1738 cm-1 (C=O ester stretching), and 1230 cm-1 (P=O stretching). The EUTF spectrum showed characteristic flavonoid peaks, with a broad O-H stretching band near 3400 cm-1 and multiple sharp peaks in the 1600-1000 cm-1 fingerprint region. For the physical mixture we see the individual peaks for all 3 simply added on top of each other indicating that there was not much of a problem with one interacting with the others. The contrary happened to the spectrum of ZL-EUTF-NPs. Zein and EUTFs broad O-H stretching band

10.57647/jnsc.2026.1603.15

has moved to a lower wavenumber and become wider, which shows that a lot of strong hydrogen bonds were formed. Following the encapsulation procedure, the amide I and II bands of zein shifted to 1656 cm^{-1} and 1545 cm^{-1}, indicating changes in the secondary structure of the protein [42]. More importantly, all the distinctive characteristic peaks of EUTF in the fingerprint region were either greatly diminished or missing in the nanoparticle spectrum.

The fact that these EUTF molecules have been successfully encapsulated inside the hydrophobic core of these nanoparticles is further evidenced by this, it would show that they are not crystalline but rather molecularly dispersed [43].

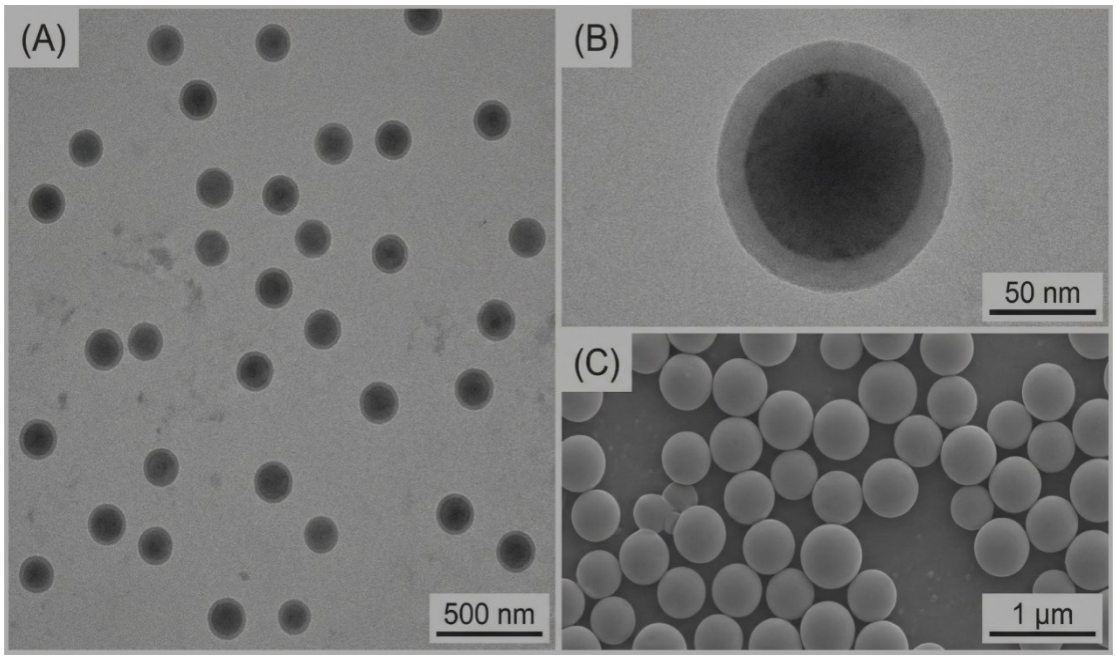

Figure 4. (A) Low-magnification TEM image, (B) High-magnification TEM image showing the core-shell structure, and (C) SEM image of the optimized ZL-EUTF-NPs

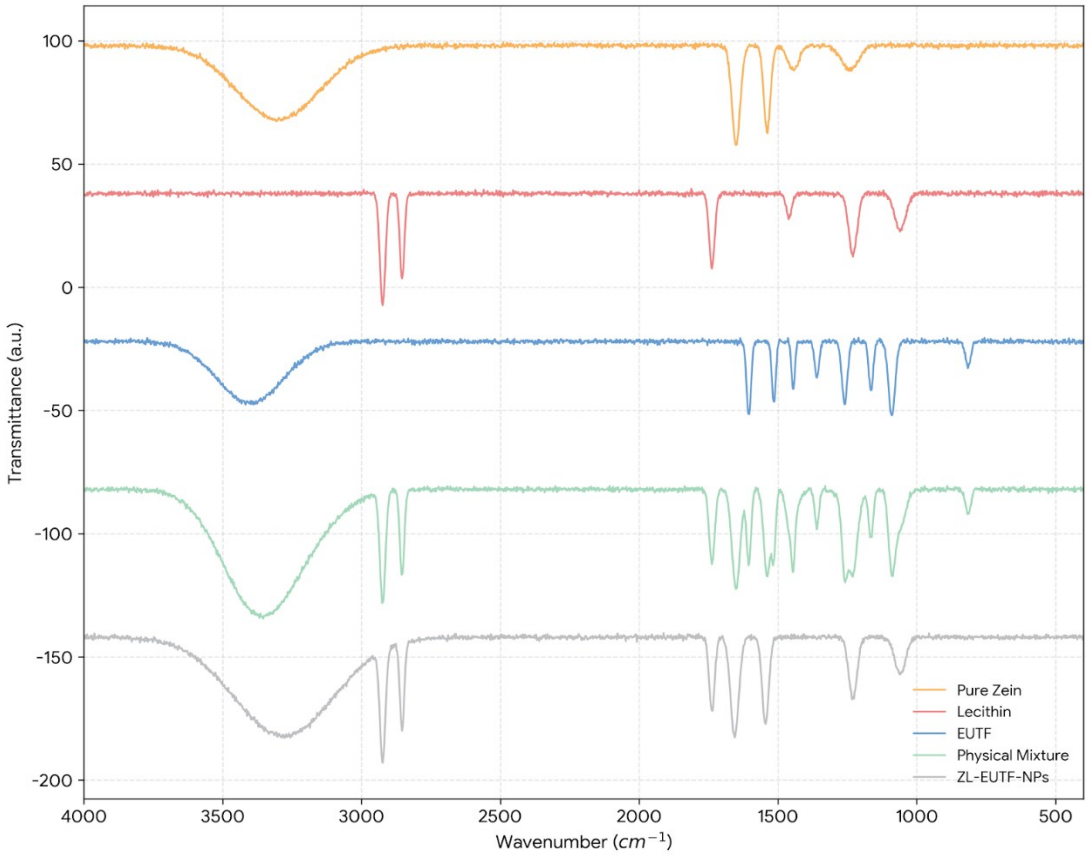

Figure 5. FTIR spectra of pure zein, lecithin, EUTF, their physical mixture, and the optimized ZL-EUTF-NPs

10.57647/jnsc.2026.1603.15

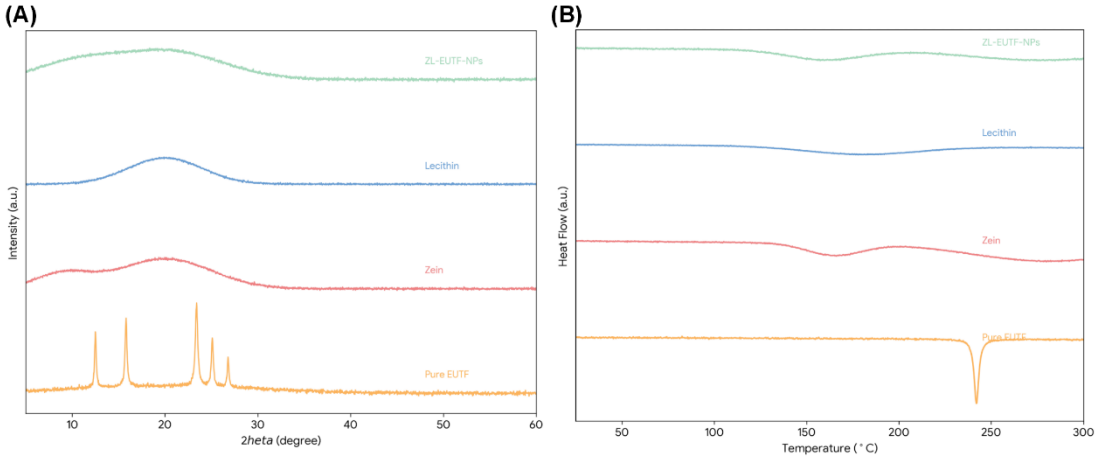

Figure 6. (A) XRD patterns of pure EUTF, zein, lecithin, and lyophilized ZL-EUTF-NPs. (B) DSC thermograms of pure EUTF, zein, lecithin, and lyophilized ZL-EUTF-NPs

XRD and DSC analyses were carried out to verify the physical state of EUTF in the nanoparticles. Fig. 6A shows the XRD pattern of pure EUTF powder, Zein and lecithin exhibited broad, amorphous halos in the analysis.The presence of numerous sharp and intense diffraction peaks indicates a highly crystalline structure. The analysis showed that zein and lecithin displayed broad, amorphous halos. The XRD pattern of the lyophilized ZL-EUTF-NPs showed a broad amorphous halo, similar to that of the empty nanoparticles, with no characteristic crystalline peaks of EUTF observed. This demonstrates that the encapsulation procedure converted the crystalline flavonoids into an amorphous form within the biopolymer matrix [44].

The DSC results shown in Fig. 6B provided supporting evidence for this finding. The DSC thermogram of pure EUTF showed a clear endothermic peak at 242°C, corresponding to its melting point. The thermogram of the ZL-EUTF-NPs showed no sign of this melting peak. The absence of the melting endotherm confirms that the EUTF is no longer in crystalline form but rather exists as a molecularly dispersed or amorphous solid solution within the nanoparticle core [45]. This amorphization is particularly beneficial because it enhances the dissolution rate and apparent solubility of poorly soluble flavonoids.

3.3. In Vitro Release and Kinetics

The release of EUTF from the nanoparticles was examined in vitro under conditions that mimic the human GI tract. Fig. 7A displays the cumulative release patterns of free EUTF, zein-EUTF nanoparticles, and the refined ZL-EUTF-NPs. Free EUTF exhibited a rapid burst release, with over 90% released within the first 2 hours in SGF. This rapid dissolution would likely lead to poor absorption and rapid clearance in vivo. In contrast, all nanoparticle formulations showed a significantly delayed and sustained release pattern. Specifically for the optimized ZL-EUTF-NPs, a very limited amount of EUTF (14.2 ± 1.8%) was released during the 2-hour incubation in SGF. This demonstrates the excellent protective effect of the zein-lecithin shell against the harsh acidic environment of the stomach, preventing premature degradation and release of the encapsulated flavonoids [46]. When the nanoparticles were transferred to SIF (pH 6.8), a sustained release was initiated. This is because zein, which is largely insoluble at low pH, begins to swell and becomes susceptible to enzymatic degradation by pancreatin in the neutral pH of the intestine [47]. The cumulative release from ZL-EUTF-NPs reached 45.5% at 6 hours and 72.8 ± 3.1% after 10 hours of total incubation. In SIF, the zein-only nanoparticles exhibited a quicker release than the zein–lecithin system, achieving nearly 80% release within 6 hours. This supports that the lecithin-enriched outer layer increases the mass-transfer resistance at the particle–medium interface and therefore acts as an additional daying the outward diffusion of EUTF and producing a more extended release profile [48]. Notably, our SIF contains both pancreatin and bile salts, and the barrier effect of lecithin is expected to be dynamic rather than static in this intestinal-like environment. Bile salts can associate with phospholipids (e.g., phosphatidylcholine in lecithin) to form bile salt–phospholipid mixed micelles/colloids, which can partially solubilize or reorganize phospholipid interfacial layers and thereby modify permeability over time [49]. In this context, we propose a time-dependent mechanism: (i) at the early stage after transfer to SIF, the lecithin shell remains sufficiently intact to provide an interfacial barrier and suppress burst release; (ii) as bile salts progressively interact with/extract lecithin into mixed colloidal structures, the shell may become more porous or thinner, increasing effective diffusivity and facilitating the sustained release observed at later time points [50]. This interpretation is consistent with the prolonged intestinal release of ZL-EUTF-NPs relative to zein-only particles and reinforces that lecithin contributes not only by ‘adding a barrier’, but also by enabling an intestinal-fluid–

responsive interfacial reorganization that modulates the release rate [51]. To analyze the release mechanism of ZL-EUTF-NPs in SIF, the experimental data were applied to four different kinetic models for evaluation (Table 3 and Fig. 7B).

The Korsmeyer–Peppas model provided the best fit, with the highest correlation coefficient ($R^2 = 0.995$). This model is often used to describe release from polymeric systems. The calculated release exponent 'n' was 0.67. For a spherical system, an 'n' value between 0.43 and 0.85 indicates an anomalous (non-Fickian) transport mechanism [52]. This suggests that the release of EUTF from the ZL-NPs is controlled by a combination of two mechanisms: Transport of the drug occurs via Fickian diffusion through the hydrated biopolymer network, alongside the erosion and degradation processes affecting the zein-lecithin polymer matrix. This intricate mechanism proves highly suitable for accomplishing sustained release within the intestinal environment [53].

3.4. Bioactivity and In Vitro Cellular Studies

The encapsulated flavonoids were evaluated for their antioxidant capacity through DPPH and ABTS assays. As shown in Figs. 8A and 8B, empty ZL-NPs exhibited negligible scavenging activity, confirming that the nanocarrier itself is not antioxidant. Free EUTF demonstrated strong radical scavenging activity, with 88.4 ± 3.1% for DPPH and 94.2 ± 2.5% for ABTS. The ZL-EUTF-NPs showed slightly lower but still very high scavenging activities of 82.1 ± 2.8% (DPPH) and 89.5 ± 3.0% (ABTS) at an equivalent EUTF concentration. This minor reduction might be due to the entrapment of some flavonoids within the nanoparticle core, making them less accessible to the radicals in the assay medium. Nevertheless, the results clearly indicate that the encapsulation process largely preserved the intrinsic antioxidant activity of the EUTF which is crucial for their intended biological function.

Table 3. Release kinetic model fitting results for EUTF release from optimized ZL-EUTF-NPs in SIF

Model	Equation	R^2	Rate Constant (k)	Release Exponent (n)
Zero-order	$Q_t = k_0 t$	0.892	5.85 h^{-1}	—
First-order	$\ln(100 - Q_t) = -k_1 t$	0.956	0.14 h^{-1}	—
Higuchi	$Q_t = k_h t^{1/2}$	0.978	21.61 $h^{-1/2}$	—
Korsmeyer–Peppas	$Q_t/Q_\infty = kt^n$	0.995	0.25 h^{-n}	0.67

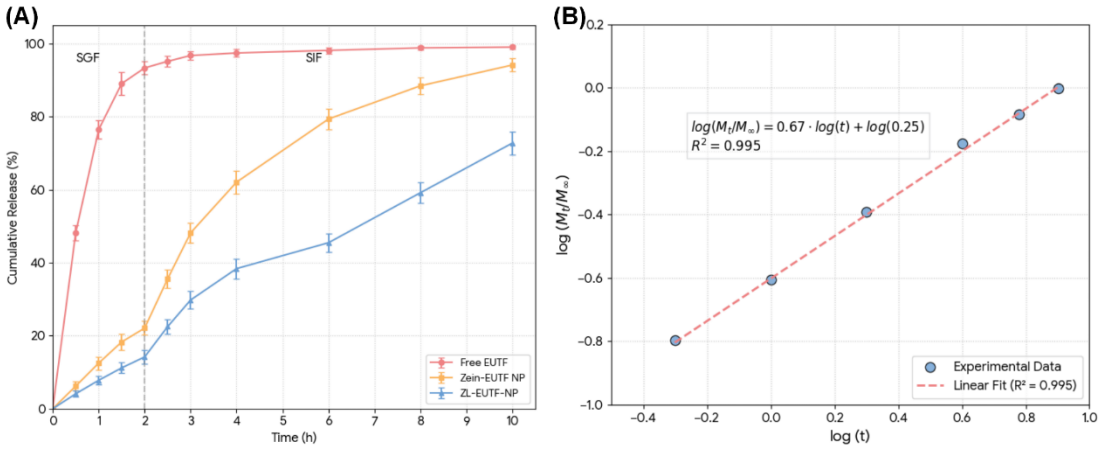

Figure 7. (A) Cumulative release patterns of free EUTF, zein-EUTF nanoparticles, and optimized ZL-EUTF nanoparticles in SGF (0–2 h) and SIF (2–10 h). Data are presented as mean ± SD (n=3). (B) The release of EUTF from optimized ZL-EUTF-NPs in SIF was analyzed using the Korsmeyer-Peppas model

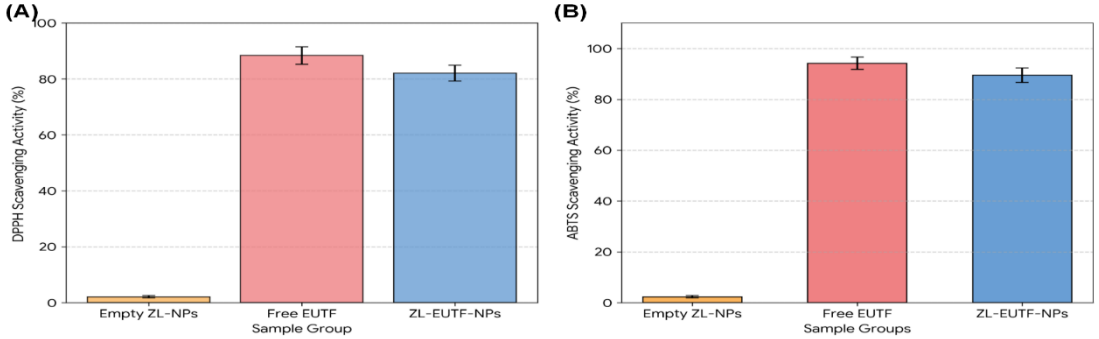

Figure 8. (A) Free EUTF, empty ZL-NPs, and ZL-EUTF-NPs exhibit DPPH radical scavenging activity. (B) Free EUTF, empty ZL-NPs, and ZL-EUTF-NPs demonstrate ABTS free radical removal activity

10.57647/jnsc.2026.1603.15

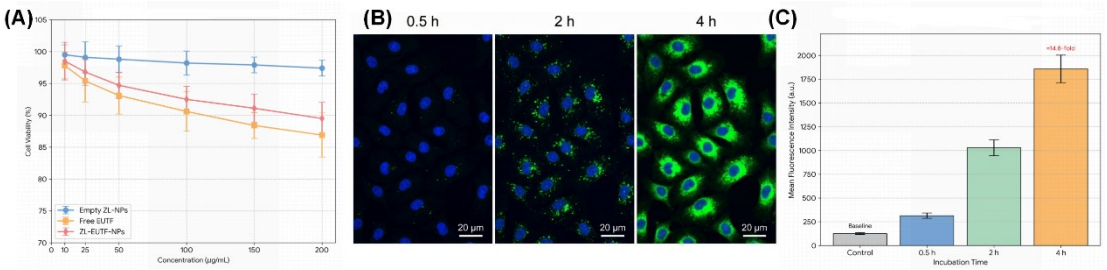

Figure 9. (A) Cytotoxicity assessment of free EUTF, empty ZL-NPs, and ZL-EUTF-NPs on Caco-2 cells after 24h incubation using the CCK-8 assay. Data are presented as mean ± SD (n=3). (B) Fluorescence microscopy images show Caco-2 cells at 0.5, 2, and 4 hours of incubation with Coumarin-6-loaded ZL-NPs. (Blue: DAPI-stained nuclei; Green: Coumarin-6-loaded NPs). Scale bar: 20 μm. (C) Time-dependent cellular uptake of Coumarin-6-loaded ZL-NPs in Caco-2 cells measured by flow cytometry

The biocompatibility of the nanocarriers is a prerequisite for their use in food and medicine. The formulations' cytotoxicity was assessed using Caco-2 cells, which serve as a typical model for the human intestinal epithelium. As shown in Fig. 9A, the empty ZL-NPs were found to be non-toxic, with cell viability remaining above 95% even at the highest tested concentration (equivalent to 1 mg/mL of biopolymers), confirming the excellent biocompatibility of the zein-lecithin carrier. Both free EUTF and ZL-EUTF-NPs exhibited low cytotoxicity, with cell viability remaining above 85% across the entire concentration range tested (10–200 μg/mL EUTF equivalent). This indicates that the developed nanoparticle system is safe for potential oral administration.

To investigate whether the nanoparticles could be internalized by intestinal cells. Cellular uptake studies, both qualitative and quantitative, were conducted using Coumarin-6 as a fluorescent marker. The fluorescence microscopy images in Fig. 9B clearly show that after incubation with Caco-2 cells, a time-dependent increase in green fluorescence was observed within the cytoplasm. Minimal fluorescence was seen at 0.5 hours, but it became much more intense at 2 and 4 hours, indicating that the cells gradually absorbed the nanoparticles over time. The fluorescence was primarily localized in the perinuclear region of the cytoplasm, suggesting an endocytic uptake pathway.

The quantitative analysis by flow cytometry (Fig. 9C) confirmed these observations. Cells treated with coumatin-6 loaded with ZL-NPs showed a notable increase in mean fluorescence intensity as time progressed, from a baseline level to a nearly 15-fold increase after 4 hours of incubation. This efficient cellular internalization is a key advantage of the nanosystem, as it can facilitate the transport of the poorly permeable flavonoids across the intestinal barrier, potentially leading to enhanced oral bioavailability.

Although the present work did not include uptake-inhibition assays, the observed time-dependent internalization can be discussed in the context of established nanoparticle uptake pathways in intestinal epithelial models. In Caco-2 cells, nanoparticle entry is commonly dominated by energy-dependent endocytosis, with contributions from clathrin-mediated endocytosis, caveolae/lipid raft-mediated uptake, and macropinocytosis depending on particle size, surface chemistry, and charge [54]. Our ZL-EUTF-NPs show a hydrodynamic diameter of ~155 nm and a strongly negative surface potential (~ −35 mV), features that typically favor endocytic internalization over passive diffusion and can bias uptake toward specific vesicular routes rather than direct membrane permeation [55]. In addition, the lecithin-enriched surface introduces phospholipid motifs that can enhance interactions with cell membranes and lipid-raft domains, providing a plausible basis for partial involvement of caveolae/lipid raft-associated pathways, while the observed perinuclear fluorescence distribution is compatible with endosome maturation and trafficking along microtubules toward the perinuclear region [54]. Similar Caco-2 studies on nanoformulations frequently report mixed contributions of clathrin-dependent endocytosis, caveolae-mediated uptake, and macropinocytosis, reinforcing that multiple routes may operate simultaneously for particles in this size regime [56].

To strengthen mechanistic certainty in future work, we will incorporate a preliminary pathway-verification design widely used in the field, including uptake comparison at 37 °C versus 4 °C (energy dependence) and pharmacological inhibition (e.g., chlorpromazine for clathrin-mediated endocytosis, genistein/filipin for caveolae/lipid raft-associated uptake, and amiloride for macropinocytosis), combined with colocalization markers for early/late endosomes and lysosomes to map intracellular fate.

The mechanistic framing above follows the broader principle that interpreting nanoparticle–cell interaction benefits from linking observed uptake phenotypes to physicochemical design rules and testable pathway hypotheses; the reviewer-suggested Accounts of Chemical Research article is valuable in this respect as a recent perspective emphasizing mechanism-guided evaluation of nanoparticle–membrane interactions [57].

3.5. Physicochemical Stability

The long-term stability of the ZL-EUTF-NPs is critical for their practical application and shelf-life. The stability of aqueous dispersions and lyophilized powders was assessed over 90 days at temperatures of 4°C, 25°C, and 40°C.

As shown in in Table 4, the nanoparticles stored as an aqueous dispersion at 4°C demonstrated excellent stability. No significant changes ($p > 0.05$) were observed in particle size, PDI, or zeta potential during the 90-day period. The flavonoid retention also remained very high, at 94.5 ± 2.6% of the initial amount. At 25°C, slight changes were observed, with the particle size increasing to 185.3 nm and flavonoid retention dropping to 85.1 ± 3.0% after 90 days. As expected, the stability was poorest at 40°C (accelerated condition). Significant aggregation occurred, with the particle size increasing to over 350 nm and the PDI exceeding 0.4, indicating a heterogeneous and unstable system. The flavonoid retention at 40°C fell sharply to 61.7 ± 4.1%, likely due to thermal degradation of the flavonoids and destabilization of the nanostructure [58]. These results confirm that refrigeration (4°C) is the optimal condition for storing the aqueous nanoparticle dispersion.

The lyophilized powder of ZL-EUTF-NPs showed excellent stability at both 4°C and 25°C. After 90 days, the powders could be easily redispersed in water to form a uniform suspension (Fig. 10). The re-dispersed nanoparticles exhibited physicochemical properties (size, PDI, zeta potential) that were nearly identical to the freshly prepared ones, indicating that Lyophilization serves as a reliable method for extending the formulation's shelf-life over an extended period.

Table 4. Physicochemical properties of ZL-EUTF-NPs after 90 days of storage as an aqueous dispersion at different temperatures (mean ± SD, n=3)

Temp. (°C)	Particle Size (nm)	PDI	Zeta Potential (mV)	Flavonoid Retention (%)
Initial (Day 0)	155.2 ± 5.2	0.18 ± 0.02	-35.6 ± 1.5	100
4°C	158.1 ± 5.5	0.19 ± 0.02	-34.9 ± 1.8	94.5 ± 2.6
25°C	185.3 ± 9.1	0.28 ± 0.03	-28.1 ± 2.2	85.1 ± 3.0
40°C	351.6 ± 25.4	0.42 ± 0.05	-15.7 ± 2.5	61.7 ± 4.1

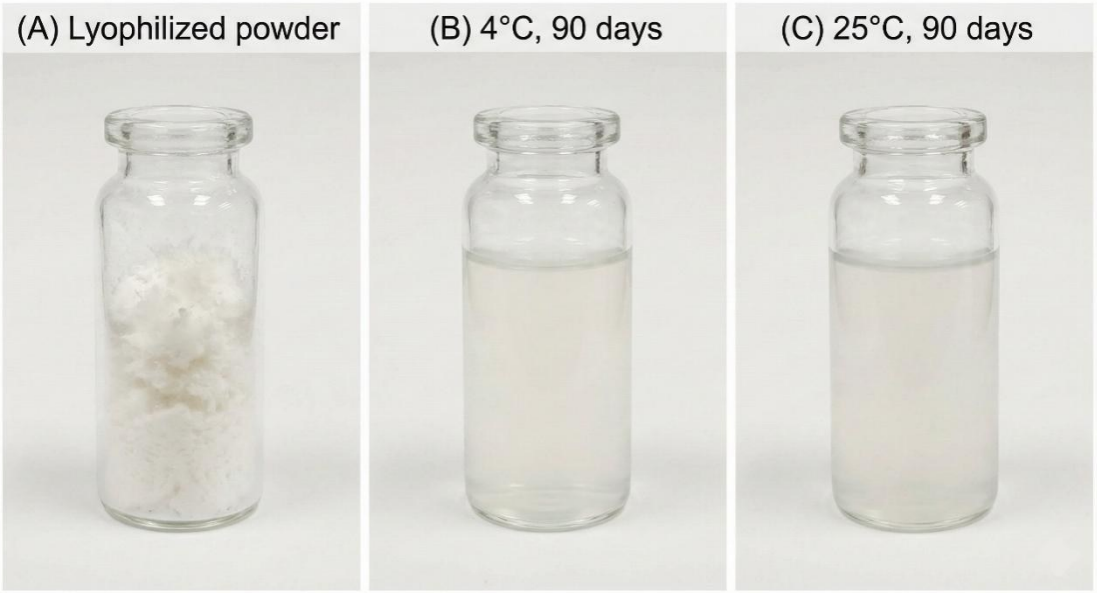

Figure 10. Visual appearance of (A) lyophilized ZL-EUTF-NP powder and its redispersed solutions after storage for 90 days at (B) 4°C and (C) 25°C

4. Conclusion

This study successfully created a new oral delivery system for total flavonoids from *Eucommia ulmoides* leaves by using zein–lecithin hybrid nanoparticles for encapsulation. The preparation of nanoparticles involved a straightforward and scalable anti-solvent co-precipitation technique, with the formulation refined to attain favorable physicochemical properties. The optimised ZL-EUTF-NPs is a spherical nuclear shell structure with a particle size of about 155 nm, a narrow distribution, a surface charge of -35.6 mV, and an encapsulation efficiency of more than 85%. Comprehensive material characterization confirmed that the crystalline flavonoids were successfully converted into an amorphous state and entrapped within the hydrophobic core of the nanoparticles through non-covalent interactions.

The developed nanocarrier demonstrated significant advantages for oral delivery. It effectively protected the encapsulated EUTF from the acidic conditions of the stomach and provided a sustained, controlled release in a

10.57647/jnsc.2026.1603.15

simulated intestinal environment, it is a joint effect of diffusion and polymer erosion. Importantly, the encapsulation process retains the high antioxidant activity of flavonoids. The nanocarrier itself was proven to be biocompatible and non-toxic to intestinal Caco-2 cells and demonstrated efficient cellular internalization, which is a crucial factor for improving oral bioavailability. Finally, the ZL-EUTF-NPs exhibited excellent long-term physicochemical stability, particularly when stored under refrigeration or as a lyophilized powder.

In general, these findings emphasise the great potential of corn-lecithin mixed nanoparticles as a powerful and effective platform for oral delivery of insoluble natural compounds (such as EUTF). This nanoencapsulation strategy offers a promising solution to enhance the stability, control the release, and potentially improve the bioavailability of *Eucommia ulmoides* flavonoids, so as to expand its application in the development of advanced functional foods, nutritional health care products and drugs.

Acknowledgements

This work was supported by the Zhejiang Province Key Discipline Construction Project of Traditional Chinese Medicine (Clinical Chinese Pharmacy) [grant NO. 2024-XK-56] and the Hangzhou Biomedicine and Health Industry Support Science and Technology Special Project (2021WJCY352). Zhejiang Province Traditional Chinese Medicine Science and Technology Plan Project (2025ZL427) and Hangzhou Municipal Key Medical Discipline (Clinical Chinese Pharmacy) [grant No. 2025HZZD17].

Author Contributions

X.-y.W. contributed to conceptualization, methodology, investigation, formal analysis, data curation, visualization, and writing – original draft. J.-w.J. contributed to methodology, investigation, formal analysis, data curation, and writing – review & editing. W.W. contributed to methodology, investigation, and data curation. Y.-l.M. contributed to resources, validation, and writing – review & editing. M.W. contributed to supervision, project administration, and funding acquisition. All authors have read and agreed to the published version of the manuscript.

Availability of Data and Materials

The data supporting the findings of this study are available from the corresponding author upon reasonable request.

Conflict of Interest

The authors declare that they have no known competing financial interests or personal relationships that could have appeared to influence the work reported in this paper.

Ethical Approval

This study does not involve human participants or living organisms, and no ethical approval was required.

References

[1] Yan, X., Li, M., Xu, X., Liu, X., Liu, F. Zein-based nano-delivery systems for encapsulation and protection of hydrophobic bioactives: A review. *Front Nutr* **9**, 999373 (2022).

[2] Luo, Y., Teng, Z., Wang, Q. Development of zein nanoparticles coated with carboxymethyl chitosan for encapsulation and controlled release of vitamin D3. *J Agric Food Chem* **60**, 836–843 (2012).

[3] de Oliveira, J.L., Campos, E.V.R., Germano-Costa, T., Lima, R., Vechia, J.F.D., Soares, S.T., de Andrade, D.J., Gonçalves, K.C., do Nascimento, J., Polanczyk, R.A., Fraceto, L.F. Association of zein nanoparticles with botanical compounds for effective pest control systems. *Pest Manag Sci* **75**, 1855–1865 (2019).

[4] Podaralla, S., Perumal, O. Preparation of zein nanoparticles by pH-controlled nanoprecipitation. *J Biomed Nanotechnol* **6**, 312–317 (2010).

[5] Kirubakaran, D. Review on emerging frontiers in medical sensing: Innovations shaping the future of healthcare. *Biomed Mater Devices* **1**, 1–15 (2025).

[6] Kirubakaran, D. Herbal remedies for Alzheimer's disease: Neuroprotective mechanisms and cognitive enhancement potential. *Digit Chin Med* **8**, 183–195 (2025).

[7] Liang, H., Zhou, B., He, L., An, Y., Lin, L., Li, Y., Liu, S., Chen, Y., Li, B. Fabrication of zein/quaternized chitosan nanoparticles for the encapsulation and protection of curcumin. *RSC Adv* **5**, 13891–13900 (2015).

[8] Dai, L., Sun, C., Wang, D., Gao, Y. Interaction between zein and lecithin in ethanol–water solution and characterization of zein–lecithin composite colloidal nanoparticles. *PLoS One* **11**, e0167172 (2016).

[9] Li, J., Zhang, Y., Jin, W., Wang, Y., Yang, L., Zhang, Z., Yan, Z. Preparation and characterization of zein–lecithin–total flavonoids nanoparticles from *Smilax glabra* and antioxidant activity in HepG2 cells. *Food Chem X* **17**, 100579 (2023).

[10] Zhang, X., Li, Y., Wu, Z., Li, J., Li, J., Deng, S., Liu, G. Development of carboxymethyl chitosan-coated zein/soy lecithin nanoparticles for the delivery of resveratrol. *Food Funct* **14**, 1636–1647 (2023).

[11] Guo, Y., Liu, P., Deng, L., Lui, C., North, M., Hu, G., Huang, Q., Zhao, Z.K., Xie, H. Molecularly engineered lignin to polyphenol via organocatalysis as an active sunscreen ingredient. *J Bioresour Bioprod* **9**, 197–210 (2024).

[12] Cedano, J., Querol, E., Mozo-Villarías, A. Amino acid hydrophobic properties in proteins derived from atomic polarities. *Eur Biophys J* **54**, 257–265 (2025).

[13] Tadele, D.T., Islam, M.S., Mekonnen, T.H. Zein-based nanoparticles and nanofibers: Co-encapsulation, characterization, and applications in food and biomedicine. *Trends Food Sci Technol* **155**, 104809 (2025).

[14] Ferreira Soares, D.C., Domingues, S.C., Viana, D.B., Tebaldi, M.L. Polymer–hybrid nanoparticles: Current advances in biomedical applications. *Biomed Pharmacother* **131**, 110695 (2020).

[15] Giteru, S.G., Ali, M.A., Oey, I. Recent progress in understanding fundamental interactions and applications of zein. *Food Hydrocoll* **120**, 106948 (2021).

[16] Rodsuwan, U., Pithanthanakul, U., Thisayakorn, K., Uttapap, D., Boonpisuttinant, K., Vatanyoopaisarn, S., Thumthanaruk, B., Rungsardthong, V. Preparation and characterization of gamma-

oryzanol-loaded zein nanoparticles with improved stability. *Food Sci Nutr* **9**, 616–624 (2021).

[17] Shazwani, S.S., Marlina, A., Misran, M. Development of nanostructured lipid carrier-loaded flavonoid-enriched *Zingiber officinale*. *ACS Omega* **9**, 17379–17388 (2024).

[18] Jan, R., Gani, A., Masarat Dar, M., Bhat, N.A. Bioactive characterization of ultrasonicated ginger and licorice freeze-dried extracts. *Ultrason Sonochem* **88**, 106048 (2022).

[19] Loeser, E. Peculiarities of mobile phases containing formic acid. *Chromatographia* **69**, 807–811 (2009).

[20] Wen, C., Zhang, J., Zhang, H., Duan, Y. New perspective on natural plant protein-based nanocarriers for bioactive ingredient delivery. *Foods* **11**, 1701 (2022).

[21] Bidyarani, N., Kumar, U. Synthesis of rotenone-loaded zein nano-formulation for plant protection against pathogenic microbes. *RSC Adv* **9**, 40819–40826 (2019).

[22] Tivano, F., Chiono, V. Zein as a renewable material for the preparation of green nanoparticles for drug delivery. *Front Biomater Sci* **2**, 1156403 (2023).

[23] H., M.S., D., C.B. Encapsulation efficiency and loading capacity of anthocyanins from *Vaccinium floribundum* in zein nanoparticles. *InfoAnalítica* **8**, 83–97 (2020).

[24] Khan, M.A., Zhou, C., Zheng, P., Zhao, M., Liang, L. Improving physicochemical stability of quercetin-loaded hollow zein particles with chitosan/pectin complex coating. *Antioxidants* **10**, 1476 (2021).

[25] Gómez-Lázaro, L., Martín-Sabroso, C., Aparicio-Blanco, J., Torres-Suárez, A.I. Assessment of in vitro release testing methods for colloidal drug carriers: The lack of standardized protocols. *Pharmaceutics* **16**, 103 (2024).

[26] Azevedo, M.A.B. Development of nanostructures for encapsulation of vitamins. PhD Thesis, Universidade do Minho (2013).

[27] Sivadasan, D., Sultan, M.H., Madkhali, O., Almoshari, Y., Thangavel, N. Polymeric lipid hybrid nanoparticles as emerging drug delivery platforms: A comprehensive review. *Pharmaceutics* **13**, 1291 (2021).

[28] Jan, R., Gani, A., Masarat Dar, M., Bhat, N.A. Bioactive characterization of ultrasonicated ginger and licorice freeze-dried extracts. *Ultrason Sonochem* **88**, 106048 (2022).

[29] Kedare, S.B., Singh, R.P. Genesis and development of DPPH method of antioxidant assay. *J Food Sci Technol* **48**, 412–422 (2011).

[30] Baek, J.-S., Tan, C.H., Ng, N.K.J., Yeo, Y.P., Rice, S.A., Loo, S.C.J. Programmable lipid–polymer hybrid nanoparticle system for sustained antibiotic delivery to bacterial biofilms. *Nanoscale Horiz* **3**, 305–311 (2018).

[31] Panta, P., Kim, D.Y., Kwon, J.S., Lee, K.W., Kim, M.S. Protein drug-loaded polymeric nanoparticles. *J Biomed Sci Eng* **7**, 825–832 (2014).

[32] Mukherjee, A., Waters, A.K., Kalyan, P., Achrol, A.S., Kesari, S., Yenugonda, V.M. Lipid–polymer hybrid nanoparticles as next-generation drug delivery platforms. *Int J Nanomedicine* **14**, 1937–1952 (2019).

[33] Liu, J., Malvandi, A., Feng, H. Comparison of cellulose nanocrystal drying via multi-frequency ultrasonics and conventional methods. *J Bioresour Bioprod* **9**, 465–485 (2024).

[34] Hallan, S.S., Sguizzato, M., Esposito, E., Cortesi, R. Challenges in the physical characterization of lipid nanoparticles. *Pharmaceutics* **13**, 549 (2021).

[35] Li, J., Zhang, Y., Jin, W., Wang, Y., Yang, L., Zhang, Z., Yan, Z. Preparation and characterization of zein–lecithin–total flavonoids nanoparticles from *Smilax glabra*. *Food Chem X* **17**, 100579 (2023).

[36] Zhang, X., Li, Y., Wu, Z., Li, J., Li, J., Deng, S., Liu, G. Development of carboxymethyl chitosan-coated zein/soy lecithin nanoparticles for resveratrol delivery. *Food Funct* **14**, 1636–1647 (2023).

[37] Bian, Y., Yang, T., Qu, Z., Zhang, T., Yang, C., Chen, G., Chen, Y., Li, S. Mechanism of charge self-reversal nano-nutrient delivery system to overcome the mucosal barrier. *Chem Eng J* **499**, 155594 (2024).

[38] Clogston, J.D., Patri, A.K. Zeta potential measurement. *Methods Mol Biol* **697**, 63–70 (2011).

[39] van 't Hag, L. Improving success rates for in meso crystallization using membrane protein mimetics. PhD Thesis, University of Melbourne (2016).

[40] Salel, S., Iyisan, B. Polymer–lipid hybrid nanoparticles as lipophilic anticancer drug carriers. *Discover Nano* **18**, 114 (2023).

[41] Aguado, R.J., Mazega, A., Tarrés, Q., Delgado-Aguilar, M. Role of electrostatic interactions of cellulose derivatives for industrial applications. *Ind Crops Prod* **201**, 116898 (2023).

[42] Loganathan, N., Sellappan, M. Design of nanosized bioflavonoids using biodegradable polymeric nanoparticles. *Int Curr Pharm J* **6**, 9–15 (2017).

[43] Ayala-Fuentes, J.C., Soleimani, M., Magaña, J.J., Gonzalez-Meljem, J.M., Chavez-Santoscoy, R.A. Hybrid inulin–soy protein nanoparticles co-loaded with epicatechin and quercetin. *Nanomaterials* **13**, 1615 (2023).

[44] Wu, M., Zhuang, Q., Lin, J., Peng, Y., Luo, F., Liu, Z., Farooq, U., Zhang, Q. Enrichment of flavonoids from *Eucommia ulmoides* leaves and antioxidant evaluation. *RSC Adv* **13**, 17406–17419 (2023).

[45] Motani, R., Gold, D.A., Carlson, S.J., Vermeij, G.J. Amniote metabolism and evolution of endothermy. *Nature* **621**, E1–E3 (2023).

[46] Lei, Y., Lee, Y. Nanoencapsulation and delivery of bioactive ingredients using zein nanocarriers. *Food Sci Biotechnol* **33**, 1037–1057 (2024).

[47] Tan, L., Yuan, G., Wang, P., Feng, S., Tong, Y., Wang, C. pH-responsive Ag-Phy@ZIF-8 nanoparticles modified by hyaluronate. *Int J Biol Macromol* **206**, 605–613 (2022).

[48] André de Almeida Campos, L., Silva Neto, A.F., Noronha, M.C.S., de Lima, M.F., Cavalcanti, I.M.F., Santos-Magalhães, N.S. Zein nanoparticles for drug delivery: Preparation methods and biological applications. *Int J Pharm* **635**, 122754 (2023).

[49] Magee, G.A., French, J., Gibbon, B., Luscombe, C. Bile salt/lecithin mixed micelles optimized for steroid solubilization. *Drug Dev Ind Pharm* **29**, 441–450 (2003).

[50] Qu, Q., Chen, L., Cheng, W., Muhire, J., Yang, A., Wang, J., Xie, M., Zhang, X., Huang, D., Xiong, R., Pei, D., Huang, C. Spontaneous compartmentalization in chitosan-based microparticles. *Chem Eng J* **477**, 147112 (2023).

[51] Sivadasan, D., Sultan, M.H., Madkhali, O., Almoshari, Y., Thangavel, N. Polymeric lipid hybrid nanoparticles as emerging drug delivery platforms. *Pharmaceutics* **13**, 1291 (2021).

[52] Ritger, P.L., Peppas, N.A. Simple equation for solute release from non-swellable devices. *J Control Release* **5**, 23–36 (1987).

[53] Qi, S., Yang, H., Fang, T., Zhang, T., Jiang, B., Manan, S., Zhang, C., Wang, P., Huang, C., Wu, W., Jin, Y. Antioxidative lignin materials attenuate T2DM progression via IRS1/PI3K/AKT axis. *J Bioresour Bioprod* **10**, 631–647 (2025).

[54] de Almeida, M.S., Susnik, E., Drasler, B., Taladriz-Blanco, P., Petri-Fink, A., Rothen-Rutishauser, B. Understanding nanoparticle endocytosis for improved targeting strategies. *Chem Soc Rev* **50**, 5397–5434 (2021).

[55] Bannunah, A.M., Vllasaliu, D., Lord, J., Stolnik, S. Mechanisms of nanoparticle internalization across intestinal epithelial models. *Mol Pharm* **11**, 4363–4373 (2014).

[56] Peng, Y., Li, X., Gu, P., Cheng, W., Zhang, R., Hu, K. Curcumin-loaded zein/pectin nanoparticles: Cellular uptake and apoptosis effects. *J Drug Deliv Sci Technol* **74**, 103497 (2022).

[57] Xiong, R., Sauvage, F., Fraire, J.C., Huang, C., De Smedt, S.C., Braeckmans, K. Photothermal nanomaterial-mediated photoporation. *Acc Chem Res* **56**, 631–643 (2023).

[58] Shraim, A.M., Ahmed, T.A., Rahman, M.M., Hijji, Y.M. Determination of total flavonoid content by aluminum chloride assay. *LWT* **150**, 111932 (2021).